PHYSICAL REVIEW B **80**, 041301(R) (2009)

Pauli spin blockade in the presence of strong spin-orbit coupling

J. Danon and Yu. V. Nazarov
Kavli Institute of NanoScience, Delft University of Technology, 2628 CJ Delft, The Netherlands

(Received 12 May 2009; revised manuscript received 18 June 2009; published 1 July 2009)

We study electron transport in a double quantum dot in the Pauli spin blockade regime in the presence of strong spin-orbit coupling. The effect of spin-orbit coupling is incorporated into a modified interdot tunnel coupling. We elucidate the role of the external magnetic field, the nuclear fields in the dots, and the spin relaxation. We find qualitative agreement with experimental observations, and we propose a way to extend the range of magnetic fields in which blockade can be observed.

DOI: 10.1103/PhysRevB.80.041301 PACS number(s): 71.70.Ej, 73.63.Kv, 72.25.−b

Blockade phenomena, whereby strong interactions between single particles affect the global transport or excitation properties of a system, are widely used to control and detect quantum states of single particles. In single electron transistors, the electrostatic interaction between electrons can block the current flow,[1] thereby enabling precise control over the number of charges on the transistor.[2] In semiconductor quantum dots, the Pauli exclusion principle can lead to a spin-selective blockade,[3] which has proven to be a powerful tool for read-out of the spin degree of freedom of single electrons.[4–8]

In this spin blockade regime, a double quantum dot is tuned such that current involves the transport cycle $(0,1)\rightarrow(1,1)\rightarrow(0,2)\rightarrow(0,1)$, (n,m) denoting a charge state with $n(m)$ excess electrons in the left(right) dot [see Fig. 1(a)]. Since the only accessible (0,2) state is a spin singlet, the current is blocked as soon as the system enters a (1,1) triplet state [Fig. 1(b)]; transport is then due to spin relaxation processes, possibly including interaction with the nuclear fields.[9] This blockade has been used in GaAs quantum dots to detect coherent rotations of single electron spins,[4,5] coherent rotations of two-electron spin states,[6] and mixing of two-electron spin states due to hyperfine interaction with nuclear spins.[7,8]

Motivated by a possibly large increase in efficiency of magnetic and electric control over the spin states,[10,11] also quantum dots in host materials with a relatively large g factor and strong spin-orbit interaction are being investigated. Very recently, Pauli spin blockade has been demonstrated in a double quantum dot defined by top gates along an InAs nanowire.[12,13] However, as compared to GaAs, spin blockade in InAs nanowire quantum dots seems to be destroyed by the strong spin-orbit coupling: significant spin blockade has been only observed at very small external magnetic fields [$\lesssim$10 mT (Ref. 12)]. An important question is whether there exists a way to extend this interval of magnetic fields. To answer that question, one first has to understand the physical mechanism behind the lifting of the blockade.

In this work we study Pauli spin blockade in the presence of strong spin-orbit mixing. We show that the only way spin-orbit coupling interferes with electron transport through a double dot is by introducing nonspin-conserving tunneling elements between the dots. This yields coupling of the (1,1) triplet states to the outgoing (0,2) singlet, thereby lifting the spin blockade. However, for sufficiently small external magnetic fields this does not happen. If the (1,1) states are not split apart by a large Zeeman energy, they will rearrange to one coupled decaying state and three blocked states. When the external field B_0 is increased, it couples the blocked states to the decaying state. As soon as this field-induced decay grows larger than the other escape rates (i.e., $B_0^2\Gamma/t^2>\Gamma_{\mathrm{rel}}$, where Γ is the decay rate of the (0,2) singlet, t the strength of the tunnel coupling, and Γ_{rel} the spin relaxation rate,[14] the blockade is lifted. Therefore, the current exhibits a dip at small fields.

The presence of two random nuclear fields in the dots (of typical magnitude $K\sim1$ mT) complicates matters since it adds another dimension to the parameter space. We distinguish two cases: if the nuclear fields are small compared to t^2/Γ, they just provide an alternative way to escape spin blockade, which may compete with spin relaxation. There is still a dip at small magnetic fields, and the current and width of the dip are determined by the maximum of Γ_{rel} and $K^2\Gamma/t^2$. In the second case, $K\gg t^2/\Gamma$, the current may exhibit either a peak or a dip, depending on the strength and orientation of the spin-orbit mixing. If there is a peak in this regime, the crossover from dip to peak takes place at $K\sim t^2/\Gamma$.

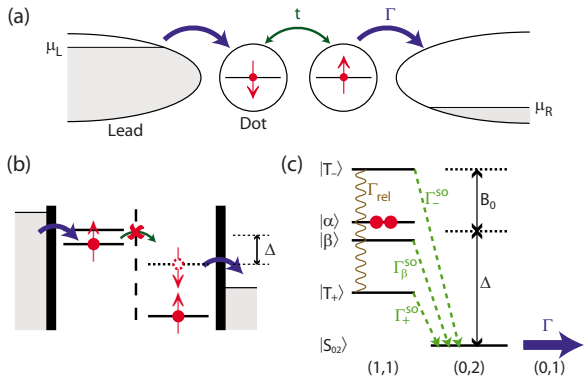

FIG. 1. (Color online) Double quantum dot in the Pauli spin blockade regime. (a) The double dot is coupled to two leads. Due to a voltage bias, electrons can only run from the left to the right lead. (b) Energy diagram assuming *spin-conserving* interdot coupling. The only accessible (0,2) state is a spin singlet: all (1,1) triplet states are not coupled to the (0,2) state and the current is blocked. (c) Energy levels and transition rates assuming *nonspin-conserving* interdot coupling. We consider the "high"-field limit and neglect the effects of the nuclear fields. Then three of the four (1,1) states can decay, leaving only one spin blockaded state $|\alpha\rangle$. Isotropic spin relaxation $\sim\Gamma_{\mathrm{rel}}$ causes transitions between all (1,1) states.

Let us now turn to our model. We describe the relative detuning of the (1,1) states and the (0,2) states by the Hamiltonian $\hat{H}_e=-\Delta|S_{02}\rangle\langle S_{02}|$, where $|S_{02}\rangle$ denotes the (0,2) spin singlet state. The energies of the four (1,1) states are further split by the magnetic fields acting on the electron spins, $\hat{H}_m=B_0(\hat{S}_L^z+\hat{S}_R^z)+\vec{K}_L\cdot\hat{\vec{S}}_L+\vec{K}_R\cdot\hat{\vec{S}}_R$, where $\hat{\vec{S}}_{L(R)}$ is the electron spin operator in the left (right) dot [for InAs nanostructures $g\sim 7$ (Ref. 15)]. We chose the z axis along $\vec{B}_0$ and included two randomly oriented effective nuclear fields $\vec{K}_{L,R}$ resulting from the hyperfine coupling of the electron spin in each dot to N nuclear spins [in InAs quantum dots $N\sim 10^5$ (see Ref. 15), yielding a typical magnitude $K\propto 1/\sqrt{N}\sim 0.6$ μeV]. We treat the nuclear fields classically, disregarding feedback of the electron spin dynamics, which could lead to dynamical nuclear spin polarization.[16]

Let us now analyze the possible effects of spin-orbit coupling. (i) It can mix up the spin and orbital structure of the electron states. The resulting states will remain Kramers doublets, thus giving no qualitative difference with respect to the common spin-up and spin-down doublets. (ii) The mixing also renormalizes the g factor that defines the splitting of the doublets in a magnetic field. This, however, is not seen provided we measure B_0 in units of energy. (iii) The coupling also can facilitate spin relaxation,[17] but this is no qualitative change either. Some of these aspects have been investigated in Ref. 18.

The only place where strong spin-orbit interaction leads to a qualitative change is in the coupling between the dots. (i) The interdot tunnel coupling provides a finite overlap of states *differing* in index of the Kramers doublet (in further discussion we refer to this index as "spin"), effectively introducing non-"spin"-conserving tunneling elements. (ii) The mutual Coulomb interaction between electrons in different dots introduces an effective spin-spin coupling scaling with B_0^2 (see Ref. 10). Both these mechanisms influence the electron spin dynamics in the system and could be responsible for lifting of the spin blockade. However, when all energy scales investigated are much smaller than the typical orbital energy splitting $E_{\rm orb}$ in the dots, the effect of the tunnel coupling dominates that of the Coulomb interaction.[10] Since most lifting effects were observed at $B_0\sim 10$ mT$\ll E_{\rm orb}$, we are working in this regime and therefore focus on the spin-orbit modified tunnel coupling.

The most general nonspin-conserving tunneling Hamiltonian for two doublet electrons in left and right states reads as $\hat{H}_t=\Sigma_{\alpha,\beta}\{t^L_{\alpha\beta}\hat{a}^\dagger_{L\alpha}\hat{a}_{R\beta}+t^R_{\alpha\beta}\hat{a}^\dagger_{R\alpha}\hat{a}_{L\beta}\}$, with α,β being the spin indices, $\hat{a}^\dagger_{L(R)}$ and $\hat{a}_{L(R)}$ are the electron creation and annihilation operators in the left (right) state, and $t^{L,R}$ are coupling matrices. We impose conditions of hermiticity and time reversibility on $\hat{H}_t$ and concentrate on the matrix elements between the (1,1) states and $|S_{02}\rangle$ in our double dot setup. In the convenient basis of orthonormal unpolarized triplet states $|T_{x,y}\rangle\equiv i^{1/2\mp 1/2}\{|T_-\rangle\mp|T_+\rangle\}/\sqrt{2}$, $|T_z\rangle\equiv|T_0\rangle$, and the (1,1) singlet $|S\rangle$, this Hamiltonian reads as

$$\hat{H}_t=i\vec{t}\cdot|\vec{T}\rangle\langle S_{02}|+t_0|S\rangle\langle S_{02}|+\text{H.c.}, \tag{1}$$

with $|\vec{T}\rangle\equiv\{|T_x\rangle,|T_y\rangle,|T_z\rangle\}$. The model therefore adds a three-vector of new coupling parameters, $\vec{t}=\{t_x,t_y,t_z\}$, to the usual spin conserving t_0, the vector being a "real" vector with respect to coordinate transformations. The degree of spin state mixing by spin-orbit interaction, and therefore the typical ratio $|\vec{t}|/t_0$, is estimated as $E_{\rm so}/E_{\rm orb}$, with $E_{\rm so}$ being the energy scale of the matrix elements in the spin-orbit interaction Hamiltonian. We assume that $E_{\rm so}\gtrsim E_{\rm orb}$ (which is believed to be the case in InAs structures), and then all four coupling parameters are generally of the same order of magnitude $t_{0,x,y,z}\sim t$. As the structure of the localized electron wave functions is very much dependent on the nanostructure design and its inevitable imperfections, the direction of $\vec{t}$ is hard to predict: we consider arbitrary directions.

We describe the electron dynamics with an evolution equation for the density matrix.[9] Next to the Hamiltonian terms, we complement the equation with (i) the rates $\sim\Gamma$ describing the decay of $|S_{02}\rangle$ and the refill to a (1,1) state and (ii) a small electron spin relaxation rate $\Gamma_{\rm rel}\ll\Gamma$. The full evolution of the electron density matrix then can be written as

$$\frac{d\hat{\rho}}{dt}=-i[\hat{H}_e+\hat{H}_m+\hat{H}_t,\hat{\rho}]+\mathbf{\Gamma}\hat{\rho}+\mathbf{\Gamma}_{\rm rel}\hat{\rho}. \tag{2}$$

Experimentally, the temperature exceeds the Zeeman energy,[12] allowing us to assume isotropic spin relaxation: each (1,1) state will transit to any of the other (1,1) states with a rate $\Gamma_{\rm rel}/3$. Explicitly, we use $\mathbf{\Gamma}_{\rm rel}\hat{\rho}=-\Gamma_{\rm rel}\hat{\rho}+\frac{1}{6}\Gamma_{\rm rel}\Sigma_{\alpha,d}\hat{\sigma}^\alpha_d\hat{\rho}\hat{\sigma}^\alpha_d$, with $\hat{\sigma}^\alpha_{L(R)}$ being the Pauli matrices in the left (right) dot.

Motivated by experimental work, we assume that the decay rate Γ of $|S_{02}\rangle$ is by far the largest frequency scale in Eq. (2), i.e., $\Gamma\gg B_0,K,t,\Gamma_{\rm rel}$ (in principle Γ can be comparable with the detuning Δ). Under this assumption, we separate the time scales and derive the effective evolution equation for the density matrix in the (1,1) subspace

$$\frac{d\hat{\rho}}{dt}=-i[\hat{H}_m+\hat{H}'_t,\hat{\rho}]-\mathbf{G}^{\rm out}\hat{\rho}+\mathbf{G}^{\rm in}\hat{\rho}+\mathbf{\Gamma}_{\rm rel}\hat{\rho}. \tag{3}$$

The decay and refill terms are now incorporated into

$$G^{\rm out}_{kl,mn}=2\{\delta_{km}T_{n2}T_{2l}+\delta_{ln}T_{k2}T_{2m}\}\Gamma/(\Gamma^2+4\Delta^2)$$

$$G^{\rm in}_{kl,mn}=\delta_{kl}T_{n2}T_{2m}\Gamma/(\Gamma^2+4\Delta^2), \tag{4}$$

where $T_{a2}\equiv\langle a|\hat{H}_t|S_{02}\rangle$. The coupling between the dots gives also rise to an exchange Hamiltonian $(H'_t)_{ij}=4T_{i2}T_{2j}\Delta/(\Gamma^2+4\Delta^2)$, with $H'_t\sim G^{\rm out}$ provided that $\Gamma\sim\Delta$. This anisotropic exchange interaction has been investigated in detail in Ref. 19. The diagonal elements of $\mathbf{G}^{\rm out}$ give us the decay rates: if we consider $|T_\pm\rangle$ and $|T_0\rangle$, the three triplet states split by an external magnetic field, we find $\Gamma^{\rm so}_\pm\equiv G^{\rm out}_{\pm\pm,\pm\pm}=2\Gamma(t_x^2+t_y^2)/(\Gamma^2+4\Delta^2)$ and $\Gamma^{\rm so}_0\equiv G^{\rm out}_{00,00}=4\Gamma t_z^2/(\Gamma^2+4\Delta^2)$, all of which are $\sim\Gamma^{\rm so}\sim t^2/\Gamma$.

Let us neglect for a moment the nuclear fields and focus on zero detuning, $\Delta=0$. This allows us to grasp qualitatively the peculiarities of the spin blockade lifting, determined by competition between the Hamiltonian ($\sim B_0$) and dissipative terms ($\sim t^2/\Gamma,\Gamma_{\rm rel}$) in Eq. (3).

At sufficiently large fields, the basis states $|T_0\rangle$ and $|S\rangle$ are aligned in energy. The spin-orbit modulated tunnel

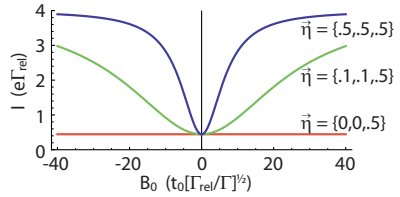

FIG. 2. (Color online) Current as a function of B_0, at $\Delta=0$, and neglecting the nuclear fields. Around zero field a dip is observed; its width depends on the magnitude and orientation of $\vec{\eta}$.

coupling then sets the difference between these states, which is best seen in a basis that mixes the states, $|\alpha\rangle \equiv \{t_0|T_0\rangle + it_z|S\rangle\}/\sqrt{t_0^2+t_z^2}$ and $|\beta\rangle \equiv \{it_z|T_0\rangle + t_0|S\rangle\}/\sqrt{t_0^2+t_z^2}$. Now $|\alpha\rangle$ is a blocked state, i.e., $G^{\rm out}_{\alpha\alpha,\alpha\alpha}=0$, while $|\beta\rangle$ decays with an effective rate $\Gamma^{\rm so}_\beta \equiv G^{\rm out}_{\beta\beta,\beta\beta}=4\Gamma(t_0^2+t_z^2)/(\Gamma^2+4\Delta^2)$. In Fig. 1(c) we give the energy levels of the five states and all transition rates in the limit of "large" external fields. It is clear that the system will spend most of its time in the state $|\alpha\rangle$. The current is determined by the spin-relaxation decay rate of this state to any unblocked state, $3\Gamma_{\rm rel}/3=\Gamma_{\rm rel}$. Let us note that if n_b states out of n states are blocked, such a decay produces on average n/n_b electrons tunneling to the outgoing lead before the system is recaptured in a blocked state. Therefore, the current is $I/e=4\Gamma_{\rm rel}$.

This picture holds until the decay rates of the three nonblocked states become comparable with $\Gamma_{\rm rel}$, which takes place at $B_0 \sim \sqrt{\Gamma^{\rm so}\Gamma_{\rm rel}}$. To understand this, let us start with considering the opposite limit, $B_0 \ll \sqrt{\Gamma^{\rm so}\Gamma_{\rm rel}}$. In this case all four (1,1) states are almost aligned in energy, and the instructive basis to work in is the one spanned by a single decaying state, $|m\rangle \equiv \{i\vec{t}\cdot|\vec{T}\rangle + t_0|S\rangle\}/\sqrt{|\vec{t}|^2+t_0^2}$, and three orthonormal states $|1\rangle$, $|2\rangle$, and $|3\rangle$ that are not coupled to $|S_{02}\rangle$. At $B_0=0$ three of the four states are blocked, and spin relaxation to the unblocked state proceeds with a rate $\Gamma_{\rm rel}/3$. A relaxation process produces on average $n/n_b=4/3$ electron transfers so that the total current is reduced by a factor of 9 in comparison with the "high"-field case, $I/e=\frac{4}{9}\Gamma_{\rm rel}$. This factor of 9 agrees remarkably well with experimental observations [see Fig. 2b in Ref. 12].

We now add a finite external field B_0 to this picture. Since $\vec{t}$ is generally not parallel to B_0, the external field will split the states $|1\rangle$, $|2\rangle$, and $|3\rangle$ in energy and mix two of them with the decaying state $|m\rangle$. This mixing results in an effective decay rate $\sim B_0^2/\Gamma^{\rm so}$, which may compete with the spin relaxation rate $\Gamma_{\rm rel}$. At $B_0 \sim \sqrt{\Gamma^{\rm so}\Gamma_{\rm rel}}$, we cross over to the "high"-field regime described above, where only one blocked state is left. Therefore, the current exhibits a dip (suppression by a factor of 9) around zero field with a width estimated as $\sqrt{\Gamma^{\rm so}\Gamma_{\rm rel}}$ (Fig. 2).

Let us now include the effects of the nuclear fields $\vec{K}_{L,R}$ on a qualitative level. If the fields are small compared to the scale t^2/Γ, their only relevant effect is to mix the states described above. This mixing creates a new possibility for decay of the blocked states, characterized by a rate $\Gamma_N \sim K^2/\Gamma^{\rm so}$. This rate may compete with spin relaxation $\sim\Gamma_{\rm rel}$ and could cause the current to scale with Γ_N and the width of the dip with K. In the opposite limit, $K \gg t^2/\Gamma$, the nuclear fields dominate the energy scales and separation of

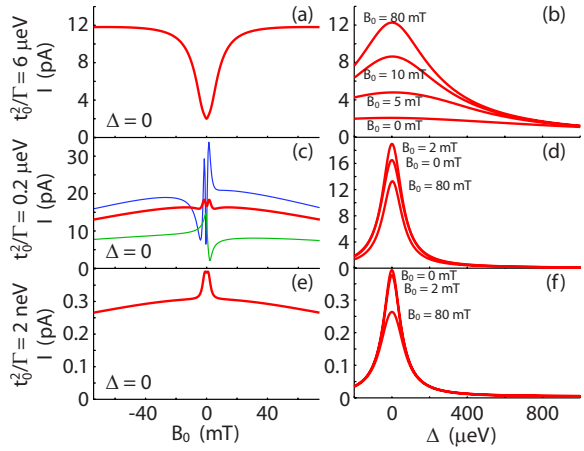

FIG. 3. (Color online) The current $I=e\rho_{22}\Gamma$ for (a) and (b) large, (c) and (d) intermediate, and (e) and (f) small tunnel coupling. The dip observed around zero field (a) disappears when $t_0^2/\Gamma \sim K$ (c) and evolves into a peak for even smaller tunnel coupling (e).

the (1,1) states at $B_0 \lesssim K$. Then, generally all four states are coupled to $|S_{02}\rangle$ on equal footing and the spin blockade is lifted. Qualitatively, this situation is similar to that without spin-orbit interaction [see Eqs. 10–12 in Ref. 9]. *Without* spin-orbit interaction, an increase in magnetic field leads to blocking of two triplet states, resulting in a current peak at zero field. *With* spin-orbit interaction, $t_{x,y}$ still couple the split-off triplets to the decaying state. Depending on the strength and orientation of $\vec{t}$, the current in the limit of "high" fields can be either smaller or larger than that at $B_0=0$, so we expect either peak or dip. If it is a peak, the transition from peak to dip is expected at $K \sim \Gamma^{\rm so}$, that is, at $t \sim \sqrt{K\Gamma}$. Indeed, such a transition has been observed upon varying the magnitude of the tunnel coupling (Fig. 2 in Ref. 12). If we assume that $K \sim 1.5$ mT and associate the level broadening observed (~ 100 μeV) with Γ, we estimate $t \sim 8$ μeV, which agrees with the range of coupling energies mentioned in Ref. 12.

Let us now support the qualitative arguments given above with explicit analytical and numerical solutions. The current through the double dot is evaluated as $I/e=\rho_{22}\Gamma$, with ρ_{22} being the steady-state probability to be in $|S_{02}\rangle$, as obtained from solving Eq. (2). We give an analytical solution for $\Delta=0$, neglecting the nuclear fields and expressing the answer in terms of the dimensionless parameter $\vec{t}/t_0=\vec{\eta}$. Under these assumptions, we find

$$I = I_{\rm max}\left(1 - \frac{8}{9}\frac{B_c^2}{B^2+B_c^2}\right), \tag{5}$$

with $B_c=2\sqrt{2}(1+|\vec{\eta}|^2)(\eta_x^2+\eta_y^2)^{-1/2}t_0\sqrt{\Gamma_{\rm rel}/\Gamma}$ and $I_{\rm max}=4e\Gamma_{\rm rel}$. The current exhibits a Lorentzian-shaped dip [see Fig. 2; compare with Fig. 2(b) in Ref. 12]. The width B_c and the limits at low and "high" fields agree with the qualitative estimations given above.

To include the effect of the two nuclear fields, we compute steady-state solutions of Eq. (2) and average over many configurations of $\vec{K}_{L,R}$.[9] In Fig. 3 we present the resulting current versus magnetic field and detuning for three different

regimes. To produce the plots we turned to concrete values of the parameters, setting $\Gamma=0.1$ meV, $\Gamma_{\mathrm{rel}}=1$ MHz, and $\vec{\eta}=0.25\times\{1,1,1\}$. We averaged over 5000 configurations of $\vec{K}_{L,R}$, randomly sampled from a normal distribution with a rms of 0.4 μeV.

In Figs. 3(a) and 3(b) we assumed large tunnel coupling, $t_0^2/\Gamma=6$ μeV so that $K\Gamma/t_0^2=0.07$ is small. In Fig. 3(a) we plot the current at $\Delta=0$, while in Fig. 3(b) we plot it versus detuning for different fixed B_0. We observe in Fig. 3(a) a Lorentzian-like dip in the current at $B_0=0$. While it looks similar to the plots in Fig. 2, the width is determined by the nuclear fields since $K\gg\Gamma_{\mathrm{rel}}$. The curve can be accurately fit with Lorentzian (5), giving $B_c=7.4K$ and $I_{\max}=0.62$ $\mathrm{K}^2\Gamma/t_0$. Figure 3(b) illustrates the unusual broadening of the resonant peak with respect to its natural width determined by Γ. The width in this case scales as $\sim t_0^2/K$ and is determined by competition of Γ^{so} and Γ_N. These plots qualitatively agree with data presented in Fig. 2(b) in Ref. 12. In Figs. 3(c) and 3(d) we present the same plots for smaller tunnel coupling, $t_0^2/\Gamma=0.2$ μeV$=0.5K$. We included in plot (c) the curves for two random nuclear field configurations: it is clear that the current strongly depends on $\vec{K}_{L,R}$, which agrees with our expectation that in the regime $\Gamma_{\mathrm{rel}}<\Gamma_N$ the current $I\propto\Gamma_N\propto K^2$. Remarkably, averaging over many configurations smoothens the sharp features at small B_0 (c.f. Ref. 9). Plots (d) exhibit no broadening with respect to Γ, in correspondence with Fig. 2a of Ref. 12. In Figs. 3(e) and 3(f) we again made the same plots for yet smaller tunnel coupling, $t_0^2/\Gamma=2$ neV$\ll K$. Since the nuclear fields now dominate the splitting of the (1,1) states, we see a peak comparable to the one in Fig. 4 of Ref. 9 surmounting a finite background current due to spin-orbit decay of the split-off triplets.

We expect our results to hold for any quantum dot system with strong spin-orbit interaction. Indeed, recent experiments on quantum dots in carbon nanotubes in the spin blockade regime[20] display the very same specific features as, e.g., a zero-field dip in the current.

Now that we understand the origin of the lifting of spin blockade, we also propose a way to extend the blockade region. If one would have a freely rotatable magnet as source of the field B_0, one would observe a large increase in width of the blockade region as soon as $\vec{B}_0$ and $\vec{t}$ are parallel. One can understand this as follows. If $\vec{t}$ effectively points along the z direction, t_x and t_y and thus $\Gamma_{\pm}^{\mathrm{so}}$ are zero: the states $|T_{\pm}\rangle$ are blocked (see Fig. 2). As $|T_{\pm}\rangle$ are eigenstates of the field B_0, this blockade could persist up to arbitrarily high fields. Since $|T_0\rangle$ and $|S\rangle$ are rotated into $|\alpha\rangle$ and $|\beta\rangle$, current will then scale in general with the antiparallel component of spin instead of only the spin singlet.

To conclude, we presented a model to study electron transport in the Pauli spin blockade regime in the presence of strong spin-orbit interaction. It reproduces all features observed in experiment, such as lifting of the spin blockade at high external fields or at low interdot tunnel coupling. We explain the mechanisms involved and identify all relevant energy scales. We also propose a simple way to extend the region of spin blockade.

We acknowledge fruitful discussions with A. Pfund, S. Nadj-Perge, S. Frolov, and K. Ensslin. This work is part of the research program of the Stichting FOM.

[1] T. A. Fulton and G. J. Dolan, Phys. Rev. Lett. **59**, 109 (1987); D. V. Averin and K. K. Likharev, J. Low Temp. Phys. **62**, 345 (1986).

[2] R. C. Ashoori, H. L. Stormer, J. S. Weiner, L. N. Pfeiffer, S. J. Pearton, K. W. Baldwin, and K. W. West, Phys. Rev. Lett. **68**, 3088 (1992).

[3] K. Ono, D. G. Austing, Y. Tokura, and S. Tarucha, Science **297**, 1313 (2002); K. Ono and S. Tarucha, Phys. Rev. Lett. **92**, 256803 (2004).

[4] F. H. L. Koppens, C. Buizert, K. J. Tielrooij, I. T. Vink, K. C. Nowack, T. Meunier, L. P. Kouwenhoven, and L. M. K. Vandersypen, Nature (London) **442**, 766 (2006).

[5] K. C. Nowack, F. H. L. Koppens, Yu. V. Nazarov, and L. M. K. Vandersypen, Science **318**, 1430 (2007).

[6] J. R. Petta, A. C. Johnson, J. M. Taylor, E. A. Laird, A. Yacoby, M. D. Lukin, C. M. Marcus, M. P. Hanson, and A. C. Gossard, Science **309**, 2180 (2005).

[7] F. H. L. Koppens, J. A. Folk, J. M. Elzerman, R. Hanson, L. H. Willems van Beveren, I. T. Vink, H. P. Tranitz, W. Wegscheider, L. P. Kouwenhoven, and L. M. K. Vandersypen, Science **309**, 1346 (2005).

[8] A. C. Johnson, J. R. Petta, J. M. Taylor, A. Yacoby, M. D. Lukin, C. M. Marcus, M. P. Hanson, and A. C. Gossard, Nature (London) **435**, 925 (2005).

[9] O. N. Jouravlev and Yu. V. Nazarov, Phys. Rev. Lett. **96**, 176804 (2006).

[10] C. Flindt, A. S. Sorensen, and K. Flensberg, Phys. Rev. Lett. **97**, 240501 (2006); M. Trif, V. N. Golovach, and D. Loss, Phys. Rev. B **75**, 085307 (2007).

[11] V. N. Golovach, M. Borhani, and D. Loss, Phys. Rev. B **74**, 165319 (2006).

[12] A. Pfund, I. Shorubalko, K. Ensslin, and R. Leturcq, Phys. Rev. Lett. **99**, 036801 (2007).

[13] A. Pfund, I. Shorubalko, R. Leturcq, and K. Ensslin, Physica E **40**, 1279 (2008).

[14] Throughout the Rapid Communication we present energies and magnetic fields in terms of frequencies. This corresponds to setting $\hbar=g\mu_B=1$.

[15] A. Pfund, I. Shorubalko, K. Ensslin, and R. Leturcq, Phys. Rev. B **76**, 161308(R) (2007).

[16] J. Danon, I. Vink, F. Koppens, K. Nowack, L. Vandersypen, and Y. Nazarov, arXiv:0902.2653 (unpublished); M. S. Rudner and L. S. Levitov, Phys. Rev. Lett. **99**, 036602 (2007).

[17] A. V. Khaetskii and Yu. V. Nazarov, Phys. Rev. B **64**, 125316 (2001).

[18] C. Romano, P. Tamborenea, and S. Ulloa, arXiv:0801.1808 (unpublished); H.-Y. Chen, V. Apalkov, and T. Chakraborty, J. Phys. Condens. Matter **20**, 135221 (2008).

[19] K. V. Kavokin, Phys. Rev. B **64**, 075305 (2001).

[20] H. O. H. Churchill, F. Kuemmeth, J. W. Harlow, A. J. Bestwick, E. I. Rashba, K. Flensberg, C. H. Stwertka, T. Taychatanapat, S. K. Watson, and C. M. Marcus, Phys. Rev. Lett. **102**, 166802 (2009).